Inorganic Chemistry
Article

Inorg. Chem. **2010**, *49*, 839–848 **839**
DOI: 10.1021/ic9013619

Effect of Ancillary Ligands on the DNA Interaction of $[Cr(diimine)_3]^{3+}$ Complexes Containing the Intercalating Dipyridophenazine Ligand

M. Scott Vandiver, E. Page Bridges, Ryan L. Koon, Alex N. Kinnaird, Jeff W. Glaeser, Jennifer F. Campbell, Chris J. Priedemann, William T. Rosenblatt, Brad J. Herbert, Sandra K. Wheeler, John F. Wheeler,* and Noel A. P. Kane-Maguire*

Department of Chemistry, Furman University, Greenville, South Carolina 29613

Received July 13, 2009

The synthesis of photoluminescent Cr(III) complexes of the type $[Cr(diimine)_2(DPPZ)]^{3+}$ are described, where DPPZ is the intercalating dipyridophenazine ligand, and diimine corresponds to the ancillary ligands bpy, phen, DMP, and TMP (where bpy = 2,2′-bipyridine, phen = 1,10-phenanthroline, DMP = 5,6-dimethyl-1,10-phenanthroline, and TMP = 3,4,7,8-tetramethyl-1,10-phenanthroline). For TMP, DMP, and phen as ancillary ligands, the complexes have also been resolved into their Λ and Δ optical isomers. A comparison of the photophysical and electrochemical properties reveal similar $^2E_g \rightarrow {}^4A_{2g}$ (O_h) emission wavelengths and lifetimes, and a variation of 110 mV in the ^2E_g excited state oxidizing power. A detailed investigation has been undertaken of ancillary ligand effects on the DNA binding of these complexes with a range of polynucleotides. For all four complexes, emission is quenched by the addition of calf thymus B-DNA, with the emission lifetime data yielding bimolecular quenching rate constants close to the diffusion controlled limit. Equilibrium dialysis studies have established a general predilection for AT base binding sites, while companion experiments with added distamycin (a selective minor groove binder) provide evidence for a minor groove binding preference. For the case of $[Cr(TMP)_2(DPPZ)]^{3+}$, concomitant equilibrium dialysis and circular dichroism measurements have demonstrated very strong enantioselective binding by the Λ optical isomer. The thermodynamics of DNA binding have also been explored via isothermal titration calorimetry (ITC). The ITC data establish that the primary binding mode for all four Cr(III) complexes is entropically driven, a result that is attributed to the highly favorable free energy contribution associated with the hydrophobic transfer of the Cr(III) complexes from solution into the DNA binding site.

Introduction

The study of the non-covalent interaction of substitution inert transition metal complexes with DNA is an area of intense current interest. This attention has been driven primarily by the desire to develop new diagnostic and therapeutic agents. Chiral $[M(diimine)_3]^{n+}$ complexes, where diimine is a polypyridyl ligand such as 2,2′-bipyridine (bpy) 1,10-phenanthroline (phen), or their derivatives, have played an important role in these investigations. This prominence has arisen in part because of their potential utility as DNA photocleavage agents via excited state redox processes.[1−9] Long-term, these $[M(diimine)_3]^{n+}$ complexes may find practical applications in the field of photodynamic therapy.[10]

To date, the most widely examined systems have been d^6 $[Ru(diimine)_3]^{2+}$ species, and their study continues to dominate the recent literature in this area.[11] Except for several notable exceptions,[8,9,11e,12] unfavorable thermodynamics,[12] and occasionally kinetic factors,[11c] preclude photoinitiated DNA damage via direct one-electron oxidation of guanine (the most readily oxidized DNA nucleobase).[13] Instead, DNA photodamage by $[Ru(diimine)_3]^{2+}$ species frequently occurs via the intermediacy of a singlet oxygen pathway.[11i,14,15] Alternatively, DNA photoactivation has been achieved by employing a tethered organic chromophore,[16] or by utilizing a sacrificial quencher to generate highly oxidizing $[Ru(diimine)_3]^{3+}$ species.[11a]

We have recently expanded the range of $[M(diimine)_3]^{n+}$ systems investigated to include the complexes $[Cr(phen)_3]^{3+}$,

*To whom correspondence should be addressed. E-mail: john.wheeler@furman.edu (J.F.W.), noel.kane-maguire@furman.edu (N.A.P.K.-M.).

(1) Murphy, C. J.; Barton, J. K. *Methods Enzymol.* **1993**, *212*, 577.
(2) Thorp, H. H. *Adv. Inorg. Chem.* **1995**, *43*, 127.
(3) Kirsch-De Mesmaeker, A.; Lecomte, J.-P.; Kelly, J. M. *Top. Curr. Chem.* **1996**, *177*, 25.
(4) Tuite, E.; Lincoln, P.; Nordén, B. *J. Am. Chem. Soc.* **1997**, *119*, 239.
(5) Errkila, K. E.; Odom, D. T.; Barton, J. K. *Chem. Rev.* **1999**, *99*, 2777.
(6) Kane-Maguire, N. A. P.; Wheeler, J. F. *Coord. Chem. Rev.* **2001**, *211*, 145.
(7) Metcalfe, C.; Thomas, J. A. *Chem. Soc. Rev.* **2003**, *32*, 215.
(8) Elias, B.; Kirsch-De Mesmaeker, A. *Coord. Chem. Rev.* **2006**, *250*, 1627.
(9) Pierard, F.; Kirsch-De Mesmaeker, A. *Inorg. Chem. Commun.* **2006**, *9*, 111.
(10) (a) DeRosa, M. C.; Crutchley, R. J. *Coord. Chem. Rev.* **2002**, *233−234*, 351. (b) Detty, M. R.; Gibson, S. L.; Wagner, S. J. *J. Med. Chem.* **2004**, *47*, 3897.

Published on Web 12/29/2009

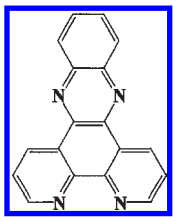

Figure 1. Intercalating DPPZ Ligand Structure.

$[Cr(bpy)_3]^{3+}$, and $[Cr(phen)_2(DPPZ)]^{3+}$,[6,17−20] (where DPPZ = dipyridophenazine, see Figure 1). For these d^3 $[Cr(diimine)_3]^{3+}$ species, quenching of the $^2E_g \rightarrow {}^4A_{2g}$ (O_h) phosphorescence signal in the presence of duplex DNA provides a valuable probe of the Cr(III)-DNA interaction. Importantly, these $[Cr(diimine)_3]^{3+}$ complexes are more powerful photooxidants than their corresponding $[Ru(diimine)_3]^{2+}$ analogues.[6,17,18,20] For example, the ^2E_g (O_h) excited state of $[Cr(bpy)_3]^{3+}$ has an oxidizing power of 1.44 V versus NHE in aqueous solution,[21] in contrast to a value of 0.84 V for the ^{3}MLCT excited state of $[Ru(bpy)_3]^{2+}$.[22] The primary reason for this enhanced oxidizing power is the markedly smaller energetic cost of ground state $M^{n+} \rightarrow M^{(n-1)+}$ reduction in the Cr(III) case.[20]

For all three $[Cr(diimine)_3]^{3+}$ listed above, their ^2E_g excited state oxidation potentials are significantly in excess of the approximate 1.2 V threshold value[13] required for the direct one-electron oxidation of guanine nucleobase. Consistent with these thermodynamic considerations, we have presented evidence that $^2E_g \rightarrow {}^4A_{2g}$ (O_h) emission quenching in the presence of DNA is associated with the direct one-electron oxidation of guanine base.[6,17,18] We have also demonstrated that these complexes are capable of causing permanent DNA photodamage.[6,20] It is noteworthy that in these latter studies the extent of photodamage was significantly greater under a nitrogen atmosphere.[20] Since cancer cells are often hypoxic,[10,11i] the increase in DNA photodamage at lower oxygen levels may provide a selectivity advantage for these $[Cr(diimine)_3]^{3+}$ reagents with regard to their future potential as phototherapeutic agents.

In our prior investigation of the interaction of $[Cr(phen)_2(DPPZ)]^{3+}$ with duplex DNA, we provided compelling evidence (including viscosity measurements) for intercalation by the DPPZ ligand into the DNA base stack.[18] As anticipated, intercalation by the DPPZ group results in a marked increase in the DNA binding constant. The remaining phen ligands serve in a secondary but important role as ancillary ligands. A systematic variation in the nature of the ancillary ligands present while maintaining DPPZ as the intercalating ligand may provide an effective avenue for fine-tuning the interaction characteristics of these $[Cr(diimine)_3]^{3+}$ species with polynucleotides. Accordingly, we describe herein the synthesis of the complexes $[Cr(bpy)_2(DPPZ)]^{3+}$, $[Cr(DMP)_2(DPPZ)]^{3+}$, and $[Cr(TMP)_2(DPPZ)]^{3+}$ (where DMP = 5,6-dimethyl-1,10-phenanthroline, and TMP = 3,4,7,8-tetramethyl-1,10-phenanthroline), and report the results of a detailed comparison of their DNA binding characteristics with those of $[Cr(phen)_2(DPPZ)]^{3+}$ (see Figures 1 and 2). These studies include the first reported investigation of the thermodynamics of DNA binding via isothermal titration calorimetry (ITC) for $[Cr(diimine)_3]^{3+}$ systems.

Experimental Section

Chemicals. Complexes of the type *cis*-$[Cr(diimine)_2Cl_2]Cl$ (diimine = bpy, phen, DMP, and TMP) were synthesized via a literature method.[23] These dichloro compounds were subsequently converted to the corresponding *cis*-$[Cr(diimine)_2(CF_3SO_3)_2]CF_3SO_3$ species by reaction with trifluormethanesulfonic acid for 24 h (while bubbling with N_2 to expel HCl gas).[24,25] The complex $[Cr(phen)_2(DPPZ)](CF_3SO_3)_3$ was prepared via a procedure we have described earlier,[25] with the sole modification being an increase in the reflux time to 27 h (UV−vis, H_2O; λ_{max}, nm (ε, M^{-1} cm^{-1}): 360 (16,600), 378 (12,700). ESI-MS: intense parent M^{3+} ion peak at a m/z value of 231.8). The dipyridophenazine ligand (Figure 1) was synthesized from 1,10-phenanthroline-5,6-dione[26] using a literature procedure,[27] and its purity was confirmed by ^{1}H NMR analysis. Preparation of the resolving agent: $(+)_D$-$K_3[Co(cysu)_3]\cdot 6H_2O$ (where cysu is the L-cysteinesulfinato ligand) was achieved utilizing the procedure developed by Dollimore and Gillard.[28]

The polynucleotides *poly*(dA-dT).*poly*(dA-dT) and *poly*(dG-dC).*poly*(dG-dC) were purchased from Amersham Biosciences,

(11) (a) Stemp, E. D. A.; Barton, J. K. *Inorg. Chem.* **2000**, *39*, 3868. (b) Önfelt, B.; Lincoln, P.; Nordén, B. *J. Am. Chem. Soc.* **2001**, *123*, 3630. (c) Delaney, S.; Pascaly, M.; Bhattacharya, P. K.; Han, K.; Barton, J. K. *Inorg. Chem.* **2002**, *41*, 1966. (d) Fu, P. K.-L.; Bradley, P. M.; van Loyen, D.; Dürr, H.; Bossman, S. H.; Turro, C. *Inorg. Chem.* **2002**, *41*, 3808. (e) Pauley, M.; Kayser, I.; Schmitz, M.; Dicato, M.; Guerzo, A. D.; Kolber, I.; Moucheron, C.; Kirsch-De Mesmaeker, A. *Chem. Commun.* **2002**, 1086. (f) Holder, A. A.; Swavey, S.; Brewer, K. J. *Inorg. Chem.* **2004**, *43*, 303. (g) Liu, F.; Wang, K.; Bai, G.; Zhang, Y.; Gao, L. *Inorg. Chem.* **2004**, *43*, 1799. (h) Rüba, E.; Hart, J. R.; Barton, J. K. *Inorg. Chem.* **2004**, *43*, 4570. (i) Chouai, A.; Wicke, S. E.; Turro, C.; Basca, J.; Dunbar, K. R.; Wang, D.; Thummel, R. P. *Inorg. Chem.* **2005**, *44*, 5996. (j) O'Donoghue, K.; Penedo, J. C.; Kelly, J. M.; Kruger, P. E. *Dalton Trans.* **2005**, 1123. (k) Xu, H.; Liang, Y.; Zhang, P.; Du, F.; Zhou, B.-R.; Wu, J.; Liu, J.-H.; Liu, Z.-G.; Ji, L.-N. *J. Biol. Inorg. Chem.* **2005**, *10*, 529. (l) Morgan, J. L.; Buck, D. P.; Turley, A. G.; Collins, J. G.; Keene, F. R. *Inorg. Chim. Acta* **2006**, *359*, 888. (m) Miao, R.; Mongelli, M. T.; Zigler, D. F.; Winkel, B. S. J.; Brewer, K. J. *Inorg. Chem.* **2006**, *45*, 10413. (n) Ma, D.-K.; Che, C.-M.; Siu, F.-U.; Yang, M.; Wong, K.-Y. *Inorg. Chem.* **2007**, *46*, 740. (o) Janaratne, T. K.; Yadav, A.; Ongeri, F.; MacDonnell, F. M. *Inorg. Chem.* **2007**, *46*, 3420. (p) Bouffier, L.; Demeunynch, M.; Dumy, P.; Moucheron, C.; Kirsch-De Mesmaeker, A. *Inorg. Chim. Acta* **2007**, *360*, 3162. (q) Puckett, C. A.; Barton, J. K. *J. Am. Chem. Soc.* **2007**, *129*, 46. (r) Ryan, G. J.; Quinn, S.; Gunnlaugsson, T. *Inorg. Chem.* **2008**, *47*, 401. (s) Sun, Y.; Lutterman, D. A.; Turro, C. *Inorg. Chem.* **2008**, *47*, 6427. (t) Nordell, P.; Westerlund, F.; Reymer, A.; El-Sagheer, A. H.; Brown, Y.; Nordén, B.; Lincoln, P. *J. Am. Chem. Soc.* **2008**, *130*, 14651. (u) Puckett, C. A.; Barton, J. K. *Biochemistry* **2008**, *47*, 11711.
(12) Lecomte, J.-P.; Kirsch-De Mesmaeker, A.; Feeney, M. M.; Kelly, J. M. *Inorg. Chem.* **1995**, *34*, 6481.
(13) Burrows, C. J.; Muller, J. G. *Chem. Rev.* **1998**, *98*, 1109.
(14) Fleisher, M. B.; Waterman, K. C.; Turro, N. J.; Barton, J. K. *Inorg. Chem.* **1986**, *25*, 3549.
(15) Mei, H.-Y.; Barton, J. K. *Proc. Natl. Acad. Sci. U.S.A.* **1988**, *85*, 1339.
(16) References 9, 11d, and 11p, and citations therein.
(17) Watson, R. T.; Desai, N.; Wildsmith, J.; Wheeler, J. F.; Kane-Maguire, N. A. P. *Inorg. Chem.* **1999**, *38*, 2683–2687.
(18) Barker, K. D.; Benoit, B. R.; Bordelon, J. A.; Davis, R. J.; Delmas, A. S.; Mytykh, O. V.; Petty, J. T.; Wheeler, J. F.; Kane-Maguire, N. A. P. *Inorg. Chim. Acta* **2001**, *322*, 74–78.
(19) Schaeper, J. P.; Nelsen, L. A.; Shupe, M. A.; Kane-Maguire, N. A. P.; Wheeler, J. F. *Electrophoresis* **2003**, *24*, 2704.
(20) Kane-Maguire, N A. P. In *Top. Curr. Chem.*; Balzani, V., Campagna, S., Eds.; Springer-Verlag: Berlin, 2007; Vol. *280*, pp 54−59.
(21) Brunschwig, B.; Sutin, N. *J. Am. Chem. Soc.* **1978**, *100*, 7568.
(22) Navin, G.; Sutin, N. *Inorg. Chem.* **1976**, *15*, 496.
(23) Burstall, F. H.; Nyholm, R. S. *J. Chem. Soc.* **1952**, 3570.
(24) Ryu, C. K.; Endicott, J. F. *Inorg. Chem.* **1988**, *27*, 2203–2214.
(25) Barker, K. D.; Barnett, K. A.; Connell, S. M.; Glaeser, J. W.; Wallace, A. J.; Wildsmith, J.; Herbert, B. J.; Wheeler, J. F.; Kane-Maguire, N. A. P. *Inorg. Chim. Acta* **2001**, *316*, 41.
(26) Dickeson, J. E.; Summers, L. A. *Aust. J. Chem.* **1970**, *23*, 1023.
(27) Hiort, C.; Lincoln, P.; Nordén, B. *J. Am. Chem. Soc.* **1993**, *115*, 3448.
(28) Dollimore, L. S.; Gillard, R. D. *J. Chem. Soc., Dalton Trans.* **1973**, 933.

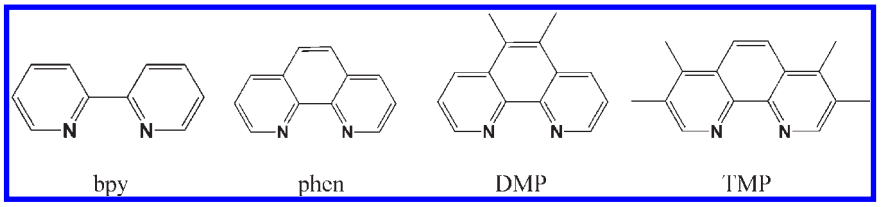

Figure 2. Ancillary Diimine Ligand Structures.

and were reconstituted in 0.1 M Tris HCl/0.1 M NaCl buffer, pH 7.4. Calf thymus B-DNA and distamycin A hydrochloride were procured from Sigma-Aldrich. The following molar absorptivities (ε) were used for concentration determinations:[29] calf thymus B-DNA, ε = 6600 M^{-1} cm^{-1}/base pair at 260 nm; *poly*(dG-dC).*poly*(dG-dC), ε = 8400 M^{-1} cm^{-1}/base pair at 254 nm; *poly*(dA-dT).*poly*(dA-dT), ε = 6600 M^{-1} cm^{-1}/base pair at 262 nm; distamycin A, ε = 37,000 M^{-1} cm^{-1} at 302 nm. Tris(hydroxymethyl)aminomethane hydrochloride (Tris-HCl) and certified ACS grade sodium chloride were purchased from Fisher Scientific. Dibenzoyl-L-tartaric acid was purchased from Aldrich Chemical, and subsequently converted to sodium dibenzoyl-L-tartrate via titration with NaOH followed by rotary evaporation to dryness. Dowex 1 × 8−50 chloride ion-exchange resin was purchased from Acros Organics. All other chemicals employed were of reagent grade quality from commercial sources, and were used without further purification. Elemental analyses (C, H, N) were performed by Midwest Microlabs.

Instrumentation. UV−visible absorption spectra were recorded using either a Cary 50 or a HP8452A diode array spectrophotometer. Steady-state emission spectral studies of the $[Cr(diimine)_2(DPPZ)]^{3+}$ products were obtained on a SPEX Fluorolog 2 fluorimeter incorporating a red sensitive Hamamatsu R928 photomultiplier. Analogous emission lifetime measurements were carried out via procedures described earlier,[30] employing a Photon Technology International N_2 laser (Model GL-3300)/dye laser (Model GL-302) system. Laser pulse excitation was at 380 nm, utilizing a BBQ dye procured from Exciton Chemical Company.

A JASCO 710 spectropolarimeter was employed for circular dichroism (CD) measurements. The experimentally measured ellipticity values ($m\theta$) at different wavelengths for optically active $[Cr(diimine)_2(DPPZ)]^{3+}$ samples were converted into their corresponding circular dichroism values ($\Delta\varepsilon$) in M^{-1} cm^{-1} units according to the equation:

$$\Delta\varepsilon = \frac{m\theta}{(32980)(b)(c)} \qquad (1)$$

where b = cell path length in cm; c = molar concentration.

Cyclic voltammetry measurements in aqueous solution were performed using a BAS 100B electrochemical analyzer, employing a Pt or glassy C working electrode, a Pt auxiliary electrode, a Ag/AgCl reference electrode, and 0.1 M KCl as supporting electrolyte. Proton NMR spectra were obtained on a Varian 300 MHz spectrophotometer. Chiral capillary electrophoresis (CCE) studies for product chemical and optical purity analysis utilized a Beckman Instruments MDQ HPCE system with UV−vis absorbance detection (monitored at 280 nm unless otherwise specified). Either potassium antimonyl-L-tartrate or sodium dibenzoyl-L-tartrate were used as the chiral additive. Uncoated fused-silica capillaries (50 μm i.d. × 360 μm o.d.) were obtained from Polymicro Technologies, cut to the desired length, and treated with 1.0 M NaOH prior to use. Injections were performed hydrodynamically for 3−8 s. All samples were prepared in deionized water (18.3 Mohm cm), and water was briefly rinsed through the capillary followed by running buffer between successive injections. To improve water solubilities, the cationic Cr(III) complexes isolated as hexafluorophosphate salts were converted to solutions of the chloride salt (using a Dowex 1 × 8−50 anion exchange resin) prior to CCE sample injections.

All electrospray ionization mass spectral (ESI-MS) data were obtained for the $[Cr(diimine)_2(DPPZ)]^{3+}$ species using a Waters ZQ LC/MS system.

Equilibrium Dialysis. Calf thymus (CT) DNA solutions were prepared in 0.1 M Tris-HCl/0.1 M NaCl buffer (pH 7.4) by sonicating in an ultrasonic bath until dissolution. CT-DNA solutions were subsequently treated with an ultrasonic probe (Ultrasonics Cell Disruptor) for three 20 s cycles (cooled between cycles) to ensure fragment uniformity. All fragments were less than 1700 base pairs based on gel electrophoresis measurements. CT DNA solutions were pre-dialyzed against 1000 mL of the Tris-HCl/NaCl buffer using a Slide-A-Lyzer cassette (Fisher Scientific) with a MW cutoff of 3,000 amu.

Cells of 0.5 or 1.0 mL capacity (Bel-Art Laboratories) on each side of a 6,000 MW cutoff membrane (Fisher Scientific) were used. Prior to loading, membranes were soaked in methanol for 10 min followed by a DI water rinse. Sample introduction was accomplished using 1 mL tuberculin syringes (Becton-Dickinson) fitted with 22-gauge standard hub blunt-end stainless steel needles (Popper).

Equilibrium dialysis experiments were carried out with excess DNA using a mole ratio of 5:1 mol DNA bases/mol $[Cr(diimine)_2(DPPZ)]^{3+}$ (measured spectrophotometrically). One chamber was loaded with *rac*-$[Cr(diimine)_2(DPPZ)]^{3+}$/DNA/0.1 M Tris HCl/0.1 M NaCl (pH 7.4) dialysis buffer (with or without distamycin), while the opposite side was loaded with an equal volume of buffer only (e.g., 500 μL). The entire cell was wrapped in aluminum foil and placed upright in the dark at room temperature for 96 h to achieve equilibrium.

UV−vis absorption spectra were collected for the retentate (initial DNA/Cr(III) side of membrane) and dialysate (buffer side of membrane) samples, allowing final $[Cr(diimine)_2(DPPZ)]^{3+}$ equilibrium concentrations to be determined post-dialysis. The presence of DNA affects the absorbance of $[Cr(diimine)_2(DPPZ)]^{3+}$ complexes (vide infra); it was thus necessary to monitor absorbance at an isosbestic wavelength (e.g., 388 nm) when measuring Cr(III) complex concentrations of retentate samples. Isosbestic wavelengths and their molar absorptivities (footnotes d-g, Table 5) were established via spectrophotometric titration of Cr(III) complexes with DNA. Circular dichroism measurements were restricted to dialysate samples, since the CD bands of the Cr(III) complexes overlap with those of B-DNA.

Isothermal Titration Calorimetry Procedures. Isothermal Titration Calorimetry (ITC) experiments were carried out using a MicroCal VP Isothermal Titration Calorimeter. Unless otherwise noted, samples were prepared using a ratio of 3:1 (mol:mol) metal complex:DNA. Concentrations of the TM complexes were generally in the concentration range of 1.5−2.7 mM with DNA concentrations ranging from 0.5 to 0.9 mM as determined

(29) Holmlin, R. E.; Stemp, E. D. A.; Barton, J. K. *Inorg. Chem.* **1998**, *37*, 29–34.
(30) Donnay, E. G.; Schaeper, J. P.; Brooksbank, R. D.; Fox, J. F.; Potts, R. G.; Davidson, R. M.; Wheeler, J. F.; Kane-Maguire, N. A. P. *Inorg. Chim. Acta* **2007**, *360*, 3272–3280.

spectrophotometrically. These complexes were prepared in 0.005 M Tris/0.05 M NaCl buffer (pH 7.4), and sonicated and filtered through a 0.45 μm syringe.

The raw ITC data accompanying the sequential injection of Cr(III) titrant into the sample cell containing calf thymus DNA exhibited a series of heat spikes (either endothermic or exothermic). The associated binding isotherm plots were then generated by integration of the individual heat peaks after correcting for heats of dilution. These binding isotherms were subsequently fit to either a single-site or two-site binding model, using the Origin software package (version 7.0) provided by Microcal. The Origin software utilizes a nonlinear least-squares algorithm which allows the DNA and Cr(III) titrant concentrations to fit the heat flow per injection to an equilibrium binding equation. This analysis procedure yields ΔH, ΔS, and K_{DNA} thermodynamic data, as well as the binding stoichiometry, n.

After each ITC experiment, 300 mL of 10% EDTA solution was drawn through the syringe and into the sample cell via the instrument cleaning apparatus followed by a second 300 mL wash with a 15 mL/300 mL Contrad 70 detergent mix. Following this wash, a third deionized water wash (300 mL) was completed, after which the instrument was capped and left with water in the sample cell.

Synthesis of *rac*-[Cr(bpy)$_2$(DPPZ)](PF$_6$)$_3$·H$_2$O. A 0.175 g (2.16×10^{-4} mol) sample of *cis*-[Cr(bpy)$_2$(CF$_3$SO$_3$)$_2$]CF$_3$SO$_3$ was combined with 0.0761 g (2.69×10^{-4} mol) of dipyridophenazine, and the mixture was refluxed in 14 mL of anhydrous CH_2Cl_2 solution while stirring for 80 min. After brief sonication, the yellow [Cr(bpy)$_2$(DPPZ)](CF$_3$SO$_3$)$_3$ product was filtered at room temperature, washed with 1 mL of CH_2Cl_2, 60 mL of ether, and suction dried. (Yield: 0.161 g). This initial product was then extracted with sonication into 9 mL of water at room temperature, and the solution filtered to remove 16 mg of undissolved material. To the filtrate was added with scratching 60 mg of NH_4PF_6 dissolved in 0.3 mL of water. The bright yellow product of [Cr(bpy)$_2$(DPPZ)](PF$_6$)$_3$ was filtered and washed with 1 mL of water, 60 mL of ether, and then suction dried. Yield: 0.090 g (38%). Anal. Calcd. for $C_{38}H_{28}N_8OP_3F_{18}Cr$: C, 41.51; H, 2.57; N, 10.19. Found: C, 41.79; H, 2.66; N, 10.08. UV−vis (H_2O; λ_{max}, nm (ε, M^{-1} cm^{-1})): 360 (15,800), 378 (12,000). ESI-MS: intense parent M^{3+} ion peak at m/z value of 215.8.

Synthesis of *rac*-[Cr(DMP)$_2$(DPPZ)](CF$_3$SO$_3$)$_3$·4H$_2$O. A mixture of 0.123 g (1.34×10^{-4} mol) of *cis*-[Cr(DMP)$_2$(CF$_3$SO$_3$)$_2$]CF$_3$SO$_3$ and 0.0516 g (1.83×10^{-4} mol) of dipyridophenazine in 5 mL of anhydrous CH_2Cl_2 was refluxed with stirring for 25.5 h. The yellow solid product was filtered at room temperature, washed with 8 mL of CH_2Cl_2, then 60 mL of ether and suction dried. Yield: 0.058 g (34%). Anal. Calcd. for $C_{49}H_{42}N_8O_{13}S_3F_9Cr$: C, 46.34: H, 3.33; N, 8.82. Found: C, 46.47; H, 3.12; N, 8.66. UV−vis (H_2O; λ_{max}, nm (ε, M^{-1} cm^{-1})): 360 (15,880), 378 (13,650). ESI-MS: intense parent M^{3+} ion peak at m/z value of 250.5.

Synthesis of *rac*-[Cr(TMP)$_2$(DPPZ)](PF$_6$)$_3$·1.5H$_2$O. A 0.200 g (2.06×10^{-4} mol) sample of *cis*-[Cr(TMP)$_2$(CF$_3$SO$_3$)$_2$]CF$_3$SO$_3$ was combined with 0.0872 g (3.09×10^{-4} mol) of dipyridophenazine, and the mixture was refluxed in 20 mL of anhydrous tetrahydrofuran solution while stirring for 9 h. The solid product of crude [Cr(TMP)$_2$(DPPZ)](CF$_3$SO$_3$)$_3$ was filtered at room temperature, and washed with 50 mL of ether and suction dried (Yield: 0.235 g). This initial product was then extracted with sonication into 30 mL of water at room temperature, and the solution filtered to remove 22 mg of undissolved material. NH_4PF_6 was added to the filtrate, and the solution cooled in the refrigerator for 1 h. The yellow product of [Cr(TMP)$_2$(DPPZ)](PF$_6$)$_3$ was then filtered, washed with 50 mL ether, and suction dried. Yield: 0.152 g (58%). Anal. Calcd. for $C_{50}H_{45}N_8O_{1.5}P_3F_{18}Cr$: C, 47.33; H, 3.57; N, 8.83. Found: C, 47.49; H, 3.92; N, 8.73. UV−vis (H_2O; λ_{max}, nm (ε, M^{-1} cm^{-1})): 360 (16,600), 378 (12,600). ESI-MS: intense parent M^{3+} ion peak at a m/z value of 269.3.

Resolution of [Cr(TMP)$_2$(DPPZ)]$^{3+}$. In a preliminary step, a solid sample of the highly water-soluble chloride salt [Cr(TMP)$_2$(DPPZ)]Cl$_3$ was isolated in 65% yield by adding an acetone solution of tetrabutylammonium chloride to a solution of *rac*-[Cr(TMP)$_2$(DPPZ)](PF$_6$)$_3$ in acetone. A representative resolution of this *rac*-[Cr(TMP)$_2$(DPPZ)]Cl$_3$ complex is described below.

A 70.9 mg (7.76×10^{-5} mol) sample of *rac*-[Cr(TMP)$_2$(DPPZ)]Cl$_3$ was dissolved in 1.0 mL of water, and powdered sodium dibenzoyl-D-tartrate resolving agent (12 mg, 2.86×10^{-5} mole) was added with scratching. After cooling in an ice bath for 5 min, the solid diastereoisomer product was filtered off. This solid was then redissolved in 1.5 mL of water, and the solution shaken with Cl^- exchange resin (Dowex 1 × 8−50) to remove the anionic resolving agent. After filtering, 2 mg of $NH_4CF_3SO_3$ was added with scratching to yield 11.8 mg of Λ-[Cr(TMP)$_2$(DPPZ)](CF$_3$SO$_3$)$_3$ (~97% optical purity).

Addition of 2 mg of $NH_4CF_3SO_3$ to the filtrate from the original diastereoisomer precipitation yielded 17.5 mg of Δ-[Cr(TMP)$_2$(DPPZ)](CF$_3$SO$_3$)$_3$ (~68% optical purity). Samples of optically pure Δ isomer were more conveniently obtained by an identical procedure to that described above, except for the use of sodium dibenzoyl-L-tartrate as the resolving agent.

Resolution of [Cr(DMP)$_2$(DPPZ)]$^{3+}$. In an initial step, the chloride salt *rac*-[Cr(DMP)$_2$(DPPZ)]Cl$_3$ was isolated in 84% yield, following the addition of tetrabutylammonium chloride to an acetone solution of [Cr(DMP)$_2$(DPPZ)](CF$_3$SO$_3$)$_3$. Then to a solution of 37.4 mg (4.02×10^{-5} mol)of *rac*-[Cr(DMP)$_2$(DPPZ)]Cl$_3$ in 1.4 mL of water was added 10 mg (2.38×10^{-5} mol) of sodium dibenzoyl-L-tartrate. After scratching the mixture several minutes at room temperature the precipitate obtained was filtered off, and washed with ether and suction dried. This procedure yielded 7.0 mg of diastereoisomer product, which after Cl^- exchange resin treatment was found to contain Δ-[Cr(DMP)$_2$(DPPZ)]$^{3+}$ of essentially 100% optical purity.

Partial Resolution of [Cr(phen)$_2$(DPPZ)]$^{3+}$. The highly water-soluble chloride salt [Cr(phen)$_2$(DPPZ)]Cl$_3$ was obtained in 86% yield by addition of tetrabutylammonium chloride to an acetone solution of *rac*-[Cr(phen)$_2$(DPPZ)](CF$_3$SO$_3$)$_3$. A representative partial resolution of this *rac*-[Cr(phen)$_2$(DPPZ)]Cl$_3$ complex using (+)$_D$-K$_3$[Co(cysu)$_3$]·6H$_2$O as resolving agent is described below.

A 53 mg (6.3×10^{-5} mol) sample of *rac*-[Cr(phen)$_2$(DPPZ)]Cl$_3$ was dissolved in 1.2 mL of water. To this solution, 47 mg (6.0×10^{-5} mol) of (+)$_D$-K$_3$[Co(cysu)$_3$]·6H$_2$O in 0.4 mL of water was added dropwise with scratching at room temperature. This afforded 15 mg of solid diastereoisomer product containing a 31% enantiomeric excess of the Λ-[Cr(phen)$_2$(DPPZ)]$^{3+}$ isomer. Subsequent cooling of the filtrate for 30 min in an ice bath resulted in a further 10 mg of diastereoisomer product containing a 19% enantiomeric excess of the Λ isomer. $NaCF_3SO_3$ was then added to the remaining filtrate, and the precipitate obtained was washed with 20 mL of ether and suction dried, yielding 10 mg of Δ-[Cr(phen)$_2$(DPPZ)](CF$_3$SO$_3$)$_3$ (of 52% optical purity).

Results and Discussion

Syntheses of *rac*-[Cr(diimine)$_2$(DPPZ)]$^{3+}$ Complexes. Good elemental analyses were obtained for the three new [Cr(diimine)$_2$(DPPZ)]$^{3+}$ species (where diimine = bpy, DMP, and TMP). Furthermore, the UV−vis absorption, emission, and electrochemical properties of all four [Cr(diimine)$_2$(DPPZ)]$^{3+}$ complexes studied are in accord with those anticipated for such compounds. However, such data do not unequivocally exclude the presence

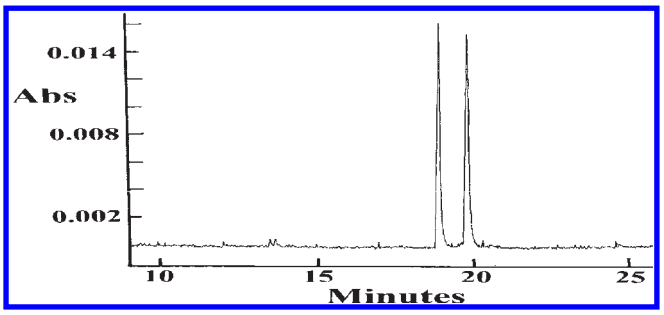

Figure 3. Electropherogram of $[Cr(DMP)_2(DPPZ)]^{3+}$ using 100 mM potassium antimonyl-L-tartrate in 25 mM phosphate buffer (pH 2.5). Conditions: 66 cm coated capillary column; field strength 24 kV; injection time 5 s at 0.5 psi; detection wavelength = 280 nm; T = 35 °C.

of fortuitous mixtures of scrambled diimine-ligand products.[30] Conclusive confirmation of the preparation of the four target Cr(III) complexes is provided by chiral capillary electrophoresis (CCE) and electrospray mass spectrometry (ESI-MS) data obtained on these compounds.

We have previously noted the value of CCE (where a chiral anion such as antimonyl-D-tartrate or dibenzoyl-L-tartrate is present in the capillary buffer medium) in assessing sample purity.[19,30−34] A representative electropherogram obtained in a CCE investigation of the target molecule $[Cr(DMP)_2(DPPZ)]^{3+}$ is shown in Figure 3. The electropherogram exhibits only two peaks (baseline separated and with equal areas), which are assigned to the Λ and Δ optical isomers of the complex. The electropherograms of the other new target complexes, $[Cr(bpy)_2(DPPZ)]^{3+}$ and $[Cr(TMP)_2(DPPZ)]^{3+}$ are of comparable quality, and are available in Supporting Information (Figure S1 and S2, respectively).

Brief ESI-MS data for all four DPPZ-containing complexes were provided in the Experimental Section. In every case, the mass spectrum is dominated by a very intense ion peak corresponding to the target M^{3+} species. A representative ESI-MS is presented in Figure 4 for the complex $[Cr(TMP)_2(DPPZ)](PF_6)_3$.

An intense ion peak is detected at a m/z ratio of 269.3, which matches the value predicted for the target molecular ion containing the Cr-52 isotope. The triply positive nature of this ion is confirmed from the m/z differences observed between the isotope satellite peaks present in the spectrum.

Resolutions of $[Cr(diimine)_2(DPPZ)]^{3+}$ Complexes. Historically, the resolution of homoleptic complexes such as $[Cr(phen)_3]^{3+}$ is conveniently carried out by first isolating a diastereoisomeric product involving the substitution labile Cr(II) species, followed by oxidation to the Cr(III) state.[35] However, this strategy is precluded for the present mixed diimine (i.e., heteroleptic) systems, since scrambling of the diimine ligands in the final Cr(III)

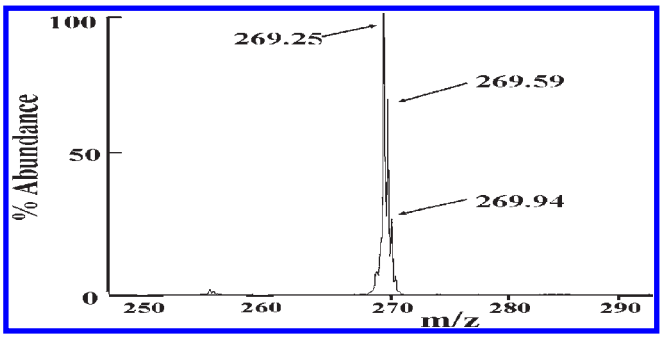

Figure 4. ESI-MS for $[Cr(TMP)_2(DPPZ)](PF_6)_3$ in acetonitrile.

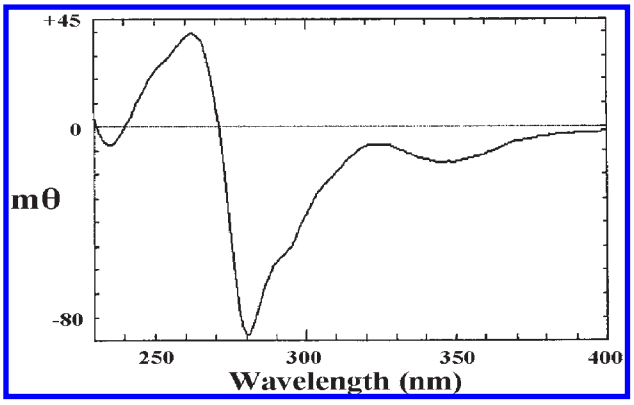

Figure 5. CD spectrum of a 1.71×10^{-5} M aqueous solution of an optically pure sample of Δ-$[Cr(TMP)_2(DPPZ)]^{3+}$ (obtained using sodium dibenzoyl-L-tartrate as resolving agent). Cell = 1 cm.

product would be very probable. Unfortunately, the diastereoisomers formed by the triply charged parent cationic complexes have high water solubilities with commonly employed anionic resolving agents. It has been necessary, therefore, to carry out resolution procedures employing very high concentrations of the racemic complexes. This requirement was met by converting the originally isolated PF_6^- or $CF_3SO_3^-$ salts to their highly water-soluble chloride salt counterparts.

Optical isomers of very high enantiomeric purity have been isolated for the complexes $[Cr(TMP)_2(DPPZ)]^{3+}$ and $[Cr(DMP)_2(DPPZ)]^{3+}$ employing dibenzoyl-L-tartrate or dibenzoyl-D-tartrate as resolving agents. However, the use of these chiral anions proved unsuccessful in the case of $[Cr(phen)_2(DPPZ)]^{3+}$, although a partial resolution was achieved utilizing the anionic Co(III) complex $(+)_D$-$[Co(cysu)_3]^{3-}$. For the bpy analogue, $[Cr(bpy)_2(DPPZ)]^{3+}$, no successful isomeric separation was detected for any of the resolving agents tested (including the antimonyl-D-tartrate anion). A representative circular dichroism (CD) spectrum for resolved $[Cr(TMP)_2(DPPZ)]^{3+}$ is shown in Figure 5, while corresponding CD spectra for resolved $[Cr(DMP)_2(DPPZ)]^{3+}$ (Figure S3) and partially resolved $[Cr(phen)_2(DPPZ)]^{3+}$ (Figure S4) are provided in Supporting Information.

In agreement with exciton coupling theory,[36] the CD spectrum of each of these complexes exhibits two major bands of opposite sign in the region of the ancillary diimine ligand $\pi \rightarrow \pi^*$ absorption band (240−320 nm). Exciton theory also predicts for these two CD bands, that

(31) Shelton, C. M.; Seaver, K. E.; Wheeler, J. F.; Kane-Maguire, N. A. P. *Inorg. Chem.* **1997**, *36*, 1532.
(32) Mytykh, O. V.; Martin, S. E.; Wheeler, J. F.; Kane-Maguire, N. A. P. *Inorg. Chim. Acta* **2000**, *311*, 143.
(33) Martin, S. E.; Connatser, R. M.; Kane-Maguire, N. A. P.; Wheeler, J. F. *Anal. Chim. Acta* **2001**, *445*, 21.
(34) Harris, J. E.; Desai, N.; Seaver, K. E.; Watson, R. T.; Kane-Maguire, N. A. P.; Wheeler, J. F. *J. Chromatogr. A* **2001**, *919*, 427.
(35) Lee, C. S.; Gorton, E. M.; Neumann, H. M.; Hunt, H. R. *Inorg. Chem.* **1966**, *5*, 1397–1399.
(36) Mason, S. F.; Peart, B. J. *J. Chem. Soc., Dalton Trans.* **1973**, 949.

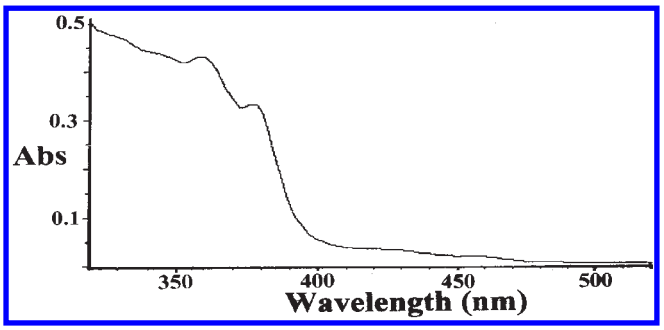

Figure 6. UV−vis absorption of $[Cr(TMP)_2(DPPZ)](PF_6)_3$ in aqueous solution.

the one at longer wavelength (280 nm, 300 nm, and 275 nm for the TMP, DMP, and phen complexes, respectively) will have a positive sign for the Λ optical isomer.[36] Thus, all three representative CD spectra depicted are for samples enriched in the Δ enantiomer. The optical purities reported in the figure captions for the three Cr(III) complexes were assessed from a chiral capillary electrophoresis (CCE) analysis of the same samples. For these Δ-enriched complexes the areas of the CE peaks for the baseline resolved Δ and Λ isomers are no longer equal, and the Δ percent optical purity (% O.P.) can be derived from the relationship:

$$\%\text{O.P.}(\Delta) = 100(\text{area } \Delta - \text{area } \Lambda)/(\text{area } \Delta + \text{area } \Lambda) \quad (2)$$

.Using these % O.P numbers and the $\Delta\varepsilon$ values experimentally observed from the CD spectra of these samples, the following absolute circular dichroism values for pure Δ and Λ isomers have been calculated:

$$[Cr(phen)_2(DPPZ)]^{3+} \quad \Delta\varepsilon(275\text{ nm}) = 152\ M^{-1}\ cm^{-1}$$

$$[Cr(DMP)_2(DPPZ)]^{3+} \quad \Delta\varepsilon(280\text{ nm}) = 171\ M^{-1}\ cm^{-1}$$

$$[Cr(TMP)_2(DPPZ)]^{3+} \quad \Delta\varepsilon(300\text{ nm}) = 155\ M^{-1}\ cm^{-1}$$

Availability of these predicted $\Delta\varepsilon$ values for optically pure samples has proven especially helpful in our subsequent investigation via equilibrium dialysis of the degree of stereoselectivity in the DNA binding of these complexes (vide infra).

UV−visible, Emission, and Electrochemical Data. The UV−visible absorption spectra in aqueous solution of the three new $[Cr(diimine)_2(DPPZ)]^{3+}$ sytems (diimine = bpy, DMP, TMP) match closely those reported earlier for the $[Cr(phen)_2(DPPZ)]^{3+}$ complex.[18] A representative spectrum is provided in Figure 6 for the species $[Cr(TMP)_2(DPPZ)]^{3+}$. A shoulder of d-d origin ($^4A_{2g} \rightarrow {}^4T_{2g}$ (O_h)) is present at approximately 420 nm, while several intense $\pi \rightarrow \pi^*$ transitions associated with the DPPZ chromophore[37] are detected in the 350−380 nm region.

The corresponding steady-state emission spectra for all four $[Cr(diimine)_2(DPPZ)]^{3+}$ sytems under study are also typical

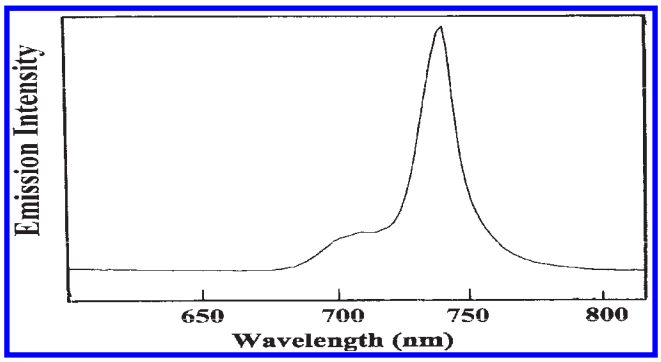

Figure 7. Steady-state emission spectrum of $[Cr(TMP)_2(DPPZ)](PF_6)_3$ in aqueous solution (wavelength of excitation = 360 nm).

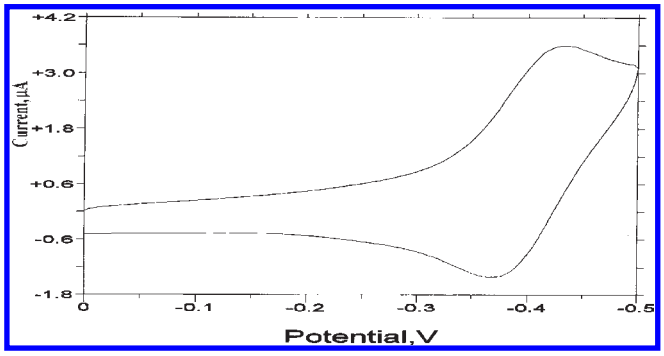

Figure 8. Cyclic voltammogram of $[Cr(bpy)_2(DPPZ)](PF_6)_3$ in 0.1 M KCl aqueous solution (vs Ag/AgCl reference electrode). Scan rate = 100 mV/s.

Table 1. Representative ITC Experimental Conditions

ITC experimental parameters	
total no. of injections	50
cell temp. (°C)	25
reference power	20 μcal/sec
initial delay	300 s
Cr(III) syringe concentration, mM	1.5−2.7 mM
DNA cell concentration, mM	0.5−0.9 mM
stirring speed	300 rpm
volume	5 μL
duration	12 s
spacing	300 s
filter period	1 s

of those observed for $[Cr(diimine)_3]^{3+}$ species,[18,25,30,38,39] and a representative spectrum is provided in Figure 7 for $[Cr(TMP)_2(DPPZ)]^{3+}$.

In Table 2 below, the wavelength maxima for the dominant $^2E_g \rightarrow {}^4A_{2g}$ (O_h) emission component are collated for all four target complexes. Also listed in Table 2 are the corresponding luminescence lifetime results obtained for air and nitrogen saturated aqueous solutions.

The cyclic voltammograms (CV) of all the complexes reported in Table 2 exhibited a reversible $[Cr(diimine)_3]^{3+}/[Cr(diimine)_3]^{2+}$ couple, from which values for the Cr^{3+}/Cr^{2+} ground state standard reduction potentials, $E^0(Cr^{3+}/Cr^{2+})$, were determined. A representative CV is shown in Figure 8 for the complex $[Cr(bpy)_2(DPPZ)]^{3+}$.

(37) Hiort, C.; Lincoln, P.; Nordén, B. *J. Am. Chem. Soc.* **1993**, *115*, 3448.

(38) Jamieson, M. A.; Serpone, N.; Hoffman *Coord. Chem. Rev.* **1981**, *39*, 121.

(39) Isaacs, M.; Sykes, A. G.; Ronco, S. *Inorg. Chim. Acta* **2006**, *316*, 3847–3854.

Table 2. Photophysical and Electrochemical Data for $[Cr(diimine)_2(DPPZ)]^{3+}$ Complexes at 24 °C[a]

	emission λ_{max}		emission lifetime			
	(nm)	(V)	air (μs)	N_2 (μs)	$E^o(Cr^{3+}/Cr^{2+})$ vs SHE (V)	$E^o(*Cr^{3+}/Cr^{2+})$ vs SHE (V)
$[Cr(bpy)_2(DPPZ)]^{3+}$	728	1.70	45	56	−0.20	1.50
$[Cr(phen)_2(DPPZ)]^{3+}$	728	1.70	54	125	−0.21	1.49
$[Cr(DMP)_2(DPPZ)]^{3+}$	728	1.70	45	169	−0.24	1.46
$[Cr(TMP)_2(DPPZ)]^{3+}$	735	1.69	33	180	−0.30	1.39

[a] Emission data were measured in aqueous solution, and 0.1 M KCl solutions were used for cyclic voltammetry experiments. Potentials vs SHE were calculated using a potential of 200 mV for the Ag/AgCl reference electrode.

A dependence of $E^0(Cr^{3+}/Cr^{2+})$ on the ancillary diimine ligand type is apparent from the data in Table 1, with the ease of Cr^{3+} ground state reduction being most favored by the presence of bpy and least favored for TMP as ancillary ligand. Of particular interest with regard to possible DNA photooxidation by $[Cr(diimine)_2(DPPZ)]^{3+}$ species (vide infra) are trends in the Cr(III) ^2E_g excited state oxidizing power, $E^0(*Cr^{3+}/Cr^{2+})$, for the four complexes investigated. These values (listed in the final column of Table 1) were estimated from the difference between the emission energies in eV units (column 3) and the ground state standard reduction potentials, $E^0(Cr^{3+}/Cr^{2+})$, provided in column 6. A variation of 110 mV is observed in the excited state oxidation potentials, with the values lying in the voltage range thermodynamically relevant for guanine base oxidation.[13]

UV−visible Titration of Cr(III) Complexes with Calf-Thymus DNA. For all four $[Cr(diimine)_2(DPPZ)]^{3+}$ complexes, the progressive addition of duplex DNA results in a pronounced hypochromism in the absorptions associated with the DPPZ $\pi \rightarrow \pi^*$ transition. Concomitant with these changes is the presence of an isosbestic point in the 380−390 nm range. A representative example is provided in Figure 9 for the case of $[Cr(bpy)_2(DPPZ)]^{3+}$ with calf thymus B-DNA. Such perturbations of the DPPZ chromophore have been previously reported for $[M(diimine)_2(DPPZ)]^{n+}$ analogues of Ru(II), Ir(III), and Co(III),[37,40,41] and are consistent with (although not definitive evidence for)[42−44] intercalation by DPPZ into the DNA base stack.

Scatchard plot analysis of these spectral changes were performed, where the data were fit to the non-cooperative binding equation of McGhee and von Hippel.[45] This procedure yielded the following DNA binding constants (K_{DNA}) for the four $[Cr(diimine)_2(DPPZ)]^{3+}$ complexes (Table 3).

The binding constants in Table 3 are comparable to that reported for $[Ru(phen)_2(DPPZ)]^{2+}$ under similar conditions.[46] The most striking result, however, is the 10-fold difference between the DNA binding constants of the Λ and Δ optical isomers of $[Cr(TMP)_2(DPPZ)]^{3+}$.

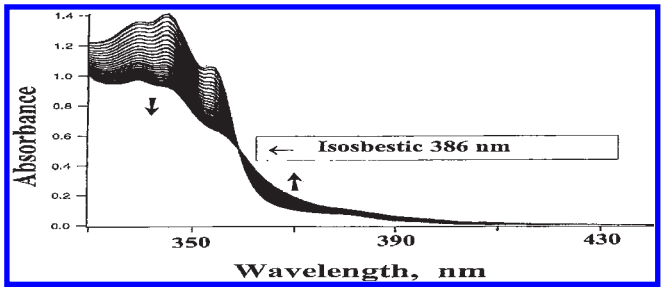

Figure 9. UV−vis spectral titration of $[Cr(bpy)_2(DPPZ)]^{3+}$ in the presence of increasing concentrations of calf thymus B-DNA in 0.05 M Tris HCl/0.1 M NaCl buffer solution (pH 7.4).

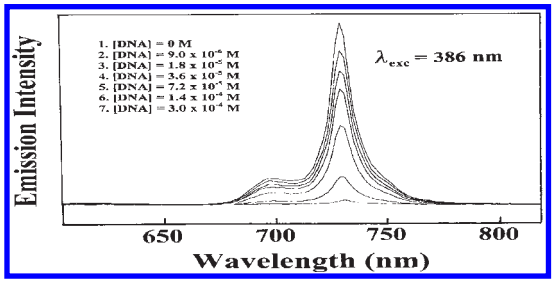

Figure 10. Steady-state emission spectrum $[Cr(bpy)_2(DPPZ)]^{3+}$ of an air-saturated 7.6×10^{-5} M solution of $[Cr(bpy)_2(DPPZ)]^{3+}$ in 0.05 M Tris-HCl buffer in the presence of increasing concentration of calf thymus B-DNA (excitation wavelength = 386 nm).

Table 3. Binding Constants with Calf Thymus B-DNA in 0.05 M Tris-HCl /0.1 M NaCl Buffer (pH 7.4)

complex	K_{DNA} (M^{-1})
$[Cr(bpy)_2(DPPZ)]^{3+}$	4.0×10^5
$[Cr(phen)_2(DPPZ)]^{3+}$	3.0×10^5
$[Cr(DMP)_2(DPPZ)]^{3+}$	1.8×10^5
rac-$[Cr(TMP)_2(DPPZ)]^{3+}$	2.8×10^5
Δ-$[Cr(TMP)_2(DPPZ)]^{3+}$	4.5×10^4
Λ-$[Cr(TMP)_2(DPPZ)]^{3+}$	5.0×10^5

This observation indicates a strong stereopreference for Λ-isomer binding for the TMP system, and is in accord with our equilibrium dialysis data (vide infra).

Quenching of Cr(III) Complex Emission by Calf-Thymus DNA. Consistent with our earlier findings for $[Cr(phen)_3]^{3+}$ and $[Cr(bpy)_3]^{3+}$,[17] the steady-state emission spectrum of all four $[Cr(diimine)_2(DPPZ)]^{3+}$ complexes in aqueous buffer solution is strongly quenched upon the sequential addition of calf thymus B-DNA. A typical example is shown in Figure 10 for the case of $[Cr(bpy)_2(DPPZ)]^{3+}$. The isosbestic wavelength of 386 nm (Figure 9) was chosen for excitation to eliminate contributions to emission quenching from a decrease in absorption related to the presence of DNA.

(40) Holmlin, R. E.; Yao, J. A.; Barton, J. K. *Inorg. Chem.* **1999**, *38*, 174.
(41) Jin, L.; Yang, P. *J. Inorg. Biochem.* **1997**, *68*, 79.
(42) Coates, C. G.; McGarvey, J. J.; Callaghan, P. L.; Coletti, M.; Hamilton, J. G. *J. Phys. Chem. B* **2001**, *105*, 730–735.
(43) Moon, S. J.; Kim, J. M.; Choi, J. Y.; Kim, S. K.; Lee, J. S.; Jang, H. G. *J. Inorg. Biochem.* **2005**, *99*, 994–1000.
(44) Lutterman, D. A.; Chouai, A.; Liu, Y.; Sun, Y.; Stewart, C. D.; Dunbar, K. R.; Turro, C. *J. Am. Chem. Soc.* **2008**, *130*, 1163.
(45) Petty, J. T.; Bordelon, J. A.; Robertson, M. E. *J. Phys. Chem. B* **2000**, *104*, 7221.
(46) Haq, I.; Lincoln, P.; Suh, D.; Nordén, B.; Chowdhry, B. Z.; Chaires, J. B. *J. Am. Chem. Soc.* **1995**, *117*, 4788.

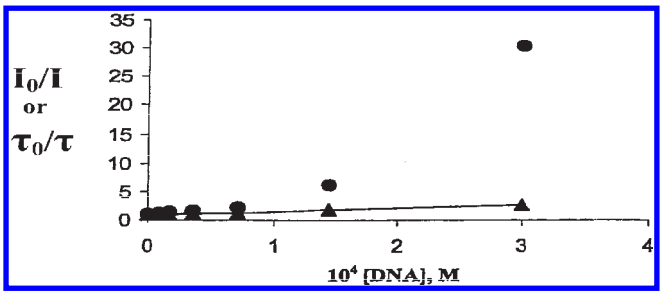

Figure 11. Stern−Volmer plots for emission quenching of an air-saturated 7.6×10^{-5} M solution of $[Cr(bpy)_2(DPPZ)]^{3+}$ in 0.05 M Tris-HCl buffer (pH 7.4) by calf thymus B-DNA: (●) steady-state emission intensity data, I_0/I; (▲) lifetime emission data, τ_0/τ.

Table 4. Bimolecular Rate Constants, k_q, for Quenching of $[Cr(diimine)_2(DPPZ)]^{3+}$ Emission by Calf Thymus B-DNA

complex	k_q (M^{-1} cm^{-1})	$E^0(*Cr^{3+}/Cr^{2+})$
$[Cr(bpy)_2(DPPZ)]^{3+}$	9.0×10^7	1.50 V
$[Cr(phen)_2(DPPZ)]^{3+}$	3.0×10^7	1.49 V
$[Cr(DMP)_2(DPPZ)]^{3+}$	3.0×10^7	1.46 V
$[Cr(TMP)_2(DPPZ)]^{3+}$	2.4×10^7	1.39 V

Emission lifetime quenching is also observed under the same conditions, and the Stern−Volmer (SV) plots for steady-state and lifetime quenching for $[Cr(bpy)_2(DPPZ)]^{3+}$ are compared in Figure 11. A straight line fit in accord with collisional quenching is observed in the lifetime SV plot, yielding a bimolecular quenching rate constant of 9.0×10^7 M^{-1} s^{-1}. The marked upward curvature of the corresponding steady-state SV plot is attributed to static quenching associated with the formation of a non-luminescent $[Cr(diimine)_3]^{3+}$/DNA ion-pair.[17,18,47] The presence of both bimolecular and static quenching precludes using the steady-state emission data in Figure 10 for obtaining accurate DNA binding constant values.

Similar DNA emission quenching behavior is observed for the other $[Cr(diimine)_2(DPPZ)]^{3+}$ complexes. Table 4 provides a collation of the bimolecular quenching rate constants (k_q) obtained from lifetime SV analyses on all four systems, as well as a listing of their corresponding ^2E_g excited state oxidation potentials.

For all four complexes, the ^2E_g excited state potentials, $E^0(*Cr^{3+}/Cr^{2+})$, are in considerable excess of the thermodynamic threshold value required for guanine base oxidation ($\sim$ 1.2 V).[13] Accordingly, the k_q value observed for the bipyridine complex is only marginally smaller than that anticipated for a diffusion controlled bimolecular process, using diffusion coefficient information available for DNA.[48,49] The analogous quenching rate constants for the three phenanthroline based systems are somewhat lower, which may suggest that the observed kinetics are influenced to some degree by steric considerations.

Equilibrium Dialysis Studies of Cr(III) Complexes with Polynucleotides. The results of equilibrium dialysis studies on the four *rac*-$[Cr(diimine)_2(DPPZ)]^{3+}$ complexes with three different polynucleotides are summarized in Table 5.

The ratios of the retentate and dialysate concentrations, [R]/[D], shown in the third column of Table 5 provide a comparative measure of the strength of DNA binding, with stronger bonding characterized by larger [R]/[D] values. From the [R]/[D] ratios observed for the three polynucleotides examined, it is apparent that all four DPPZ complexes exhibit a significant binding preference for AT base sequences (this preference being especially pronounced for the bipyridine system).

For the case of CT DNA, studies were also carried out where distamycin A was added as an extra component in the initial *rac*-$[Cr(diimine)_2(DPPZ)]^{3+}$/DNA/buffer mixture. Distamycin A is a strongly AT selective minor groove binder, with a large duplex DNA binding constant. As such, it has been used as a competitive binding agent to determine the relative affinity of drugs for minor groove binding.[50] For all four DPPZ systems, the presence of distamycin results in a marked decrease in the [R]/[D] ratio. This observed binding inhibition provides persuasive evidence for a predisposition for minor groove binding by these DPPZ complexes.

The stereoselectivity of complex binding was assessed from an analysis of the circular dichroism (CD) and UV−visible absorption spectra of the dialysate solutions. The CD values ($\Delta\varepsilon$) shown for dialysate solutions in the fourth column of Table 5 are for the longer wavelength band component associated with the diimine $\pi \rightarrow \pi^*$ chromophore (see footnote h). From exciton theory,[36] a negative sign for this component can be attributed to the presence of an excess of the Δ optical isomer in the dialysate (and thus a DNA binding preference for the Λ isomer). The corresponding % optical purity values are based on a comparison of the observed $\Delta\varepsilon$ values for dialysate samples with those calculated earlier for optically pure samples (152, 171, and 155 M^{-1} cm^{-1} for the phen, DMP, and TMP complexes, respectively).

The data in columns four and five of Table 5 reveal a striking dependence of binding stereospecificity on the steric bulk and/or hydrophobicity of the ancillary diimine ligand present. In the case of the bipyridine system, no chiral discrimination is evident. In marked contrast, a strong and very strong Λ isomer binding predilection are observed when phenanthroline and TMP are the ancillary ligands, respectively.[51] This Λ isomer preference is maintained for all three polynucleotides examined, but is exhibited most prominently with AT base sequences. A contrasting situation arises in the case of DMP as the ancillary ligand. Only a very small enantiomeric preference for the Λ isomer is detected for CT DNA, while no detectable selectivity was apparent for *poly*(dA·dT)·*poly*(dA·dT). However, a clear chirality preference for Δ-$[Cr(DMP)_2(DPPZ)]^{3+}$ is evident when *poly*(dG·dC)·*poly*(dG·dC) is the polynucleotide employed. To our knowledge, this latter observation is the first reported example of a Cr(III) diimine complex exhibiting a Δ isomer binding preference with DNA.

Taken overall, these dialysis results demonstrate that binding stereoselectivities of such Cr(III) complexes display strong responses to relatively modest changes in

(47) Demas, J. N.; Addington, J. W. *J. Am. Chem. Soc.* **1974**, *96*, 3663.
(48) (a) Carter, M. T.; Bard, A. J. *J. Am. Chem. Soc.* **1987**, *109*, 7528. (b) Carter, M. T.; Rodriquez, M.; Bard, A. J. *J. Am. Chem. Soc.* **1989**, *111*, 8901.
(49) Welch, T. W.; Corbett, A. H.; Thorp, H. H. *J. Phys. Chem.* **1995**, *99*, 11757.
(50) Holmlin, R. E.; Stemp, E. D. A.; Barton, J. K. *Inorg. Chem.* **1998**, *37*, 29.
(51) Interestingly, this Λ isomer binding selectivity is the reverse of that observed for the analogous $[Ru(phen)_2(DPPZ)]^{2+}$ under comparable conditions.[52]

Table 5. Dialysis Results for *rac*-$[Cr(diimine)_2(DPPZ)]^{3+}$ Complexes Equilibrated 96 h with Duplex DNA[a]

complex	DNA type	[R]/[D][b]	dialysate $\Delta\varepsilon$[g]	% optical purity
$[Cr(bpy)_2DPPZ]^{3+}$	CT DNA	5.5	ND[h]	ND
	CT DNA/distamycin	1.3	ND	ND
	poly(dA·dT)	19.8	ND	ND
	poly(dG·dC)	3.3	ND	ND
$[Cr(phen)_2DPPZ]^{3+}$	CT DNA	5	−44.2	29%
	CT DNA/distamycin	1.3	−15.3	10%
	poly(dA·dT)	7.4	−44.1	29%
	poly(dG·dC)	3.2	ND	ND
$[Cr(DMP)_2DPPZ]^{3+}$	CT DNA	5	−4.1	2%
	CT DNA/distamycin	1.5	ND	ND
	poly(dA·dT)	9.3	ND	ND
	poly(dG·dC)	3.1	27	16%
$[Cr(TMP)_2DPPZ]^{3+}$	CT DNA	3.1	−96.2	62%
	CT DNA/distamycin	1.5	−22	14%
	poly(dA·dT)	3.9	−112	72%
	poly(dG·dC)	1.8	−45.6	30%

[a]All experiments were conducted with a molar ratio of DNA base/*rac*-$[Cr(diimine)_3]^{3+}$ of 5:1 in 0.1 M Tris HCl/0.1 M NaCl buffer (pH 7.4). [b] Retentate [R] and dialysis [D] concentrations were determined using the wavelengths and corresponding molar absorptivities noted in foonotes (d)−(g). The molar absorptivities employed for retentate concentration calculations are those associated with the isosbestic wavelength observed in Cr(III)/DNA titrations. [c] $[Cr(bpy)_2(DPPZ)]^{3+}$: ε_{386} = 6788 M^{-1} cm^{-1} [R]; ε_{360} = 15,820 M^{-1} cm^{-1} [D]. [d] $[Cr(phen)_2(DPPZ)]^{3+}$: ε_{388} = 5935 M^{-1} cm^{-1} [R]; ε_{360} = 16,600 M^{-1} cm^{-1} [D]. [e] $[Cr(DMP)_2(DPPZ)]^{3+}$: ε_{388} = 7404 M^{-1} cm^{-1} [R]; ε_{360} = 15,880 M^{-1} cm^{-1} [D]. [f] $[Cr(TMP)_2(DPPZ)]^{3+}$: ε_{388} = 6934 M^{-1} cm^{-1} [R]; ε_{360} = 16,600 M^{-1} cm^{-1} [D]. [g] The $\Delta\varepsilon$ values reported are those calculated from an analysis of the CD spectra of dialysate samples at the wavelengths 275 nm, 280 nm, and 300 nm for the phen, DMP, and TMP complexes, respectively. [h] ND = non-detectable.

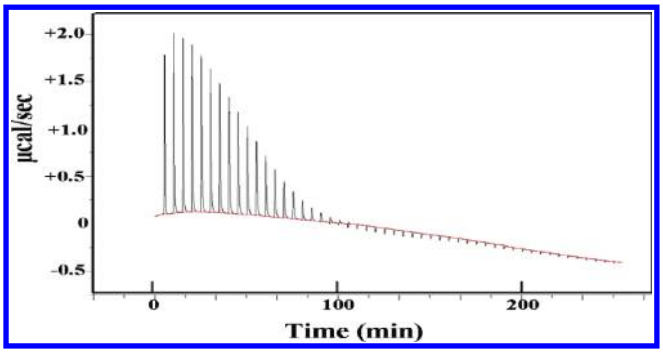

Figure 12. Raw ITC data for the titration of 0.76 mM calf thymus DNA with 2.28 mM $[Cr(TMP)_2(DPPZ)]^{3+}$ at 25 °C in 5 mM Tris HCl/50 mM NaCl at pH 7.4 (for the remaining conditions see Table 1).

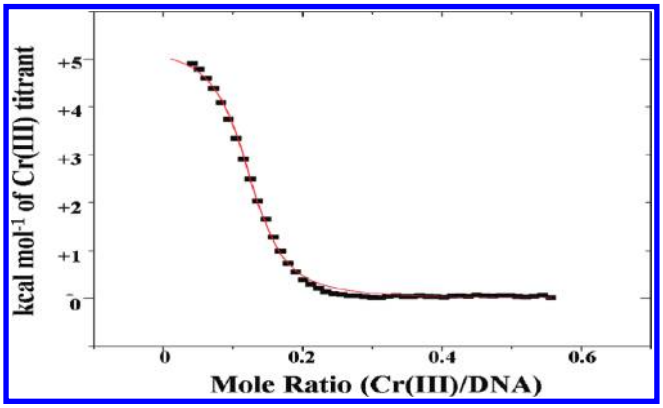

Figure 13. Corresponding binding isotherm for the ITC study at 25 °C of $[Cr(TMP)_2(DPPZ)]^{3+}$ with calf thymus B-DNA.

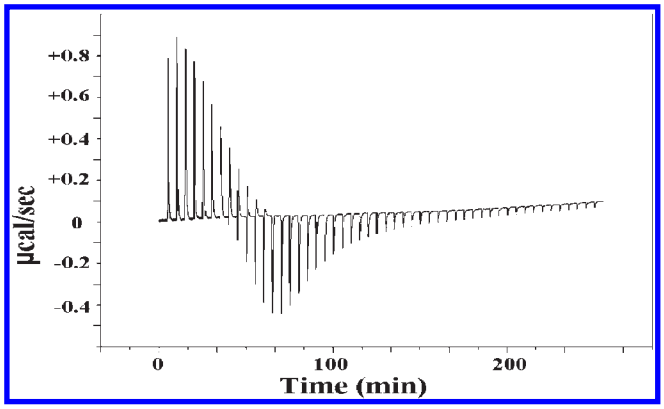

Figure 14. Raw ITC data for the titration of 0.90 mM calf thymus DNA with 2.7 mM $[Cr(phen)_2(DPPZ)]^{3+}$ at 25 °C in 5 mM Tris HCl/50 mM NaCl at pH 7.4 (for the remaining conditions see Table 1).

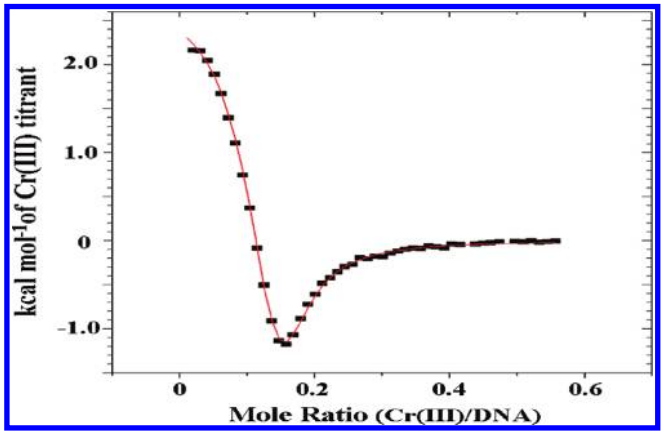

Figure 15. Corresponding binding isotherm from an ITC study at 25 °C of $[Cr(phen)_2(DPPZ)]^{3+}$ with calf thymus B-DNA.

the nature of the ancillary ligands present and the polynucleotide utilized.

Isothermal Titration Calorimetry Studies of Cr(III) Complexes with Calf- Thymus DNA. Although the noncovalent interaction of $[M(diimine)_3]^{n+}$ complexes with DNA has been the subject of extensive investigation,[1−9] information on the binding thermodynamics have been largely restricted to equilibrium constant measurements. Isothermal titration calorimetry (ITC) is a powerful technique for obtaining not only binding constants (K_{DNA}) and binding stoichiometries (n), but also important data on the relative significance of enthalpic

Table 6. Thermodynamic Parameters for Cr(III) DPPZ Complexes Binding to Calf Thymus DNA at 25 °C Obtained via ITC[b]

Cr(III) complex[a]	ΔH_1 (cal/mol)	ΔS_1 (cal/(mol K))	K_{DNA} (M^{-1})	n[c]
$[Cr(bpy)_2(DPPZ)]^{3+}$ (4)	1969 ± 138	32.9 ± 1.1	(6.6 ± 3.4) x10^5	0.16
$[Cr(phen)_2(DPPZ)]^{3+}$ (4)	3182 ± 259	37.5 ± 1.4	(8.2 ± 4.0) x10^5	0.14
$[Cr(DMP)_2(DPPZ)]^{3+}$ (2)	3474 ± 85	36.9 ± 0	(3.3 ± 0.4) x10^5	0.13
$[Cr(TMP)_2(DPPZ)]^{3+}$ (3)	5448 ± 250	42.6 ± 0.5	(2.1 ± 0.6) x10^5	0.14

[a] The number of titrations run for each complex are given in parentheses. [b] The thermodynamic values reported for each complex are the average of multiple runs, and the error values presented are the standard deviations (the error values for individual runs provided by the Origin curve-fitting program were of comparable magnitude). [c] n = binding stoichiometry = mol bound Cr(III)/mol DNA base pairs.

versus entropic factors associated with substrate/DNA interactions. Although very little thermodynamic data of this latter type are presently available for $[M(diimine)_3]^{n+}$ systems,[11k,52,53] access to such information should provide valuable information for the more rational design of potential drug candidates.

We report here the results of an ITC investigation of the four racemic $[Cr(diimine)_2(DPPZ)]^{3+}$ complexes with calf thymus DNA at 25 °C. To our knowledge, these are the first such studies for $[Cr(diimine)_3]^{3+}$ systems. The raw ITC data plots display the heat absorbed or released (in μcal/s) following each sequential addition of $[Cr(diimine)_2(DPPZ)]^{3+}$ titrant to a calf thymus DNA solution. The plot obtained for $[CrTMP)_2(DPPZ)]^{3+}$ is shown in Figure 12, and clearly demonstrates the presence of a single, significantly endothermic DNA binding term. The associated integrated binding isotherm plot (corrected for heats of dilution effects) is presented in Figure 13. Also shown is the best fit to this binding isotherm using a single-site binding model, from which values for ΔH, ΔS, K_{DNA}, and n (the binding stoichiometry) were extracted.

The analogous raw ITC and binding isotherm plots for $[Cr(phen)_2(DPPZ)]^{3+}$ are provided in Figure 14 and Figure 15, respectively. In addition to a strong primary endothermic binding term reminiscent of the TMP system, a weaker exothermic heat component is observed later in the titration. In this case, the binding isotherm was fit using a two-site model, yielding thermodynamic data for both binding sites. A secondary exothermic term is also evident in the binding isotherms for $[Cr(bpy)_2(DPPZ)]^{3+}$ and to a lesser extent for $[Cr(DMP)_2(DPPZ)]^{3+}$ (see Supporting Information, Figure S5 and Figure S6, respectively).

The thermodynamic data obtained for the secondary binding site in the bpy, phen, and DMP systems have large error limits, and are not presented here. However, it is noted that in addition to binding being modestly exothermic, this secondary mode is also characterized by weakly positive entropies and by equilibrium constants, K_{DNA}, an order of magnitude less than that for the primary endothermic binding mode.

A discussion of trends in thermodynamic profiles with changes in ancillary ligand can be undertaken with more confidence for the dominant binding mode, because of the higher quality of the data. These data are provided in Table 6 for the four Cr(III) complexes investigated.

The thermodynamic data in Table 6 establish that the primary binding mode for all four Cr(III) complexes is entropically driven, with ΔH and ΔS both positive in every instance. Although intercalating drugs often bind to DNA with negative enthalpic and entropic terms, our present results match closely those reported by Chaires and co-workers for the related $[Ru(phen)_2(DPPZ)]^{2+}$ complex.[52] They rationalized their results as due to the highly favorable free energy contribution associated with the hydrophobic transfer of the large aromatic Ru(II) complex from solution into the DNA binding site.

Hydrophobic interactions[52,54,55] also provide an attractive explanation for the data on our Cr(III) systems, an interpretation that receives additional support from the trends observed in enthalpy values with changes in ancillary ligand. Inspection of the data in Table 6 reveals a marked increase in the endothermic enthalpic term as the ancillary ligand progresses from bpy to TMP—an observation in accord with the increased bulkiness and hydrophobic character of this ligand.

Finally, the DNA binding constants listed in Table 6 appear to be in reasonable agreement with those obtained independently via UV−visible titration methods under slightly different conditions (Table 3). However, it should be noted that because of the inherently different titration protocols used, absorbance titrations more exclusively provide data on the highest affinity site than do corresponding ITC studies. As a result, UV−visible titration data are in general considered to provide more reliable primary binding constant data for systems exhibiting multiple binding modes. A more detailed understanding of both the primary and secondary DNA binding modes is the focus of an ongoing temperature dependent ITC investigation, including comparative data for Λ and Δ optical isomers.

Acknowledgment. The authors gratefully acknowledge the support of Beckman Scholars Program and the National Science Foundation (NSF-REU) for their support of this work. This publication was also made possible by NIH Grant P20 RR-016461 from the National Center for Research Resources (NIH-SC-BRIN). Support from the Furman Advantage program is also appreciated.

Supporting Information Available: Electropherograms for $[Cr(bpy)_2(DPPZ)]^{3+}$ and $[Cr(TMP)_2(DPPZ)]^{3+}$ (Figures S1 and S2, respectively), circular dichroism spectra of optically pure Δ-$[Cr(DMP)_2(DPPZ)]^{3+}$ and partially resolved Δ-$[Cr(phen)_2(DPPZ)]^{3+}$ (Figures S3 and S4, respectively), and binding isotherms from ITC studies with CT DNA for $[Cr(bpy)_2(DPPZ)]^{3+}$ and $[Cr(DMP)_2(DPPZ)]^{3+}$ (Figures S5 and S6, respectively). This material is available free of charge via the Internet at http://pubs.acs.org.

(52) Haq, I.; Lincoln, P.; Suh, D.; Norden, B.; Chowdhry, B. Z.; Chaires, J. B. *J. Am. Chem. Soc.* **1995**, *117*, 4788.
(53) Satyanarayana, S.; Dabrowiak, J. C.; Chaires, J. B. *Biochemistry* **1993**, *32*, 2573.
(54) Chaires, J. B. *Biopolymers* **1997**, *44*, 201.
(55) Holdgate, G. A. *BioTechniques* **2001**, *31*, 164.